



Tradeoff of CO₂ and CH₄ emissions from global peatlands under water-table drawdown

Yuanyuan Huang^{1,2}✉, Phillipe Ciais¹, Yiqi Luo³, Dan Zhu¹, Yingping Wang^{1,2}, Chunjing Qiu¹, Daniel S. Goll¹, Bertrand Guenet⁴, David Makowski⁵, Inge De Graaf^{6,7}, Jens Leifeld⁸, Min Jung Kwon¹, Jing Hu^{9,10} and Laiye Qu^{11,12}

Water-table drawdown across peatlands increases carbon dioxide (CO₂) and reduces methane (CH₄) emissions. The net climatic effect remains unclear. Based on global observations from 130 sites, we found a positive (warming) net climate effect of water-table drawdown. Using a machine-learning-based upscaling approach, we predict that peatland water-table drawdown driven by climate drying and human activities will increase CO₂ emissions by 1.13 (95% interval: 0.88–1.50) Gt yr⁻¹ and reduce CH₄ by 0.26 (0.14–0.52) GtCO₂-eq yr⁻¹, resulting in a net increase of greenhouse gas of 0.86 (0.36–1.36) GtCO₂-eq yr⁻¹ by the end of the twenty-first century under the RCP8.5 climate scenario. This drops to 0.73 (0.2–1.2) GtCO₂-eq yr⁻¹ under RCP2.6. Our results point to an urgent need to preserve pristine and rehabilitate drained peatlands to decelerate the positive feedback among water-table drawdown, increased greenhouse gas emissions and climate warming.

Covering only ~3% of the Earth's land surface, peatlands store one-third of the global soil carbon¹. Peat is formed through a slow accumulation of detritus with litter input exceeding decomposition rates in waterlogged environments. In pristine peatlands, a shallow water table or permanently waterlogged condition causes oxygen deficiency, allowing the accumulation of organic matter over millennia. These anaerobic conditions favour methanogenesis, and peatlands thus act as a global source of methane (CH₄) of around 0.8 GtCO₂-eq yr⁻¹ (1 Gt = 10¹⁵ g) (ref.²). CH₄ is a greenhouse gas (GHG) with a global warming potential that is 25 times that of carbon dioxide (CO₂) over a 100-year time horizon³. Pristine peatlands are a sink of CO₂ of around 0.4 GtCO₂ yr⁻¹ at the global scale². The balance between CO₂ sinks and CH₄ emissions determines the net climatic impact of peatlands. This balance is highly sensitive to changes in hydrology, particularly the water-table position that regulates aerobic versus anaerobic conditions in the soil column and therefore the production and consumption processes of CO₂ and CH₄ in the soil profile⁴.

Human-induced drainage, over-extraction of groundwater and climate drying have substantially altered peatland hydrology and resulted in a widespread downward movement of water tables. Around 51 Mha of the world's peatlands have been drained for agriculture or forestry⁵. Water-table drawdown and associated land subsidence have been observed in warm and wet peat regions such as Indonesia, Malaysia, Thailand, Florida (Everglades); in specific summer dry regions such as California (Sacramento delta) and Israel (Lake Hula)^{6,7}; and in temperate countries like the Netherlands⁸. Peatlands across Europe have also undergone substantial and widespread drying in recent centuries⁹. Globally,

drainage and subsequent conversion of natural peatlands to agriculture and forestry are estimated to emit 0.31–3.38 GtCO₂-eq yr⁻¹ GHGs (see Supplementary Table 1 for a summary of GHG emissions on degraded peatlands). These estimates rely on peatland area and GHG emission factors. Both the area and emission factors and their upscaling are highly uncertain^{5,10,11}. It is unclear to what extent and how water-table drawdown directly regulates changes of GHG emissions as it is challenging to separate compounding effects of other variables such as land clearing and carbon input to the soil from the new land use types.

Field manipulation experiments provide the opportunity to quantify the direct impact of lowering the water table on peatland GHG emissions. We compiled data from 376 pairs of data points measuring net ecosystem exchange of CO₂ (NEE), 532 pairs for CH₄ emissions, 209 pairs for gross primary production (GPP) and 407 pairs for ecosystem respiration (or soil respiration in the absence of live plants, RES). The data were extracted from 130 field sites as documented in 96 publications (Supplementary Fig. 1). NEE is jointly controlled by soil and vegetation (NEE = GPP + RES). Lowering of water tables is expected to accelerate peat decomposition and soil CO₂ release by exposing carbon-rich upper soil layers to oxygen. However, some studies measured either a decrease or no change in decomposition rates¹². Individual studies have also observed vegetation CO₂ uptake (GPP) increase, decrease and have no significant change when the water table was lowered. Correspondingly, the sign of NEE changes in response to water-table drawdown varies among studies (Supplementary Fig. 11). However, studies mostly reported reductions in CH₄ emissions by lowering the water table (Supplementary Fig. 11). With highly uncertain soil emissions and

¹Laboratoire des Sciences du Climat et de l'Environnement, LSCE/IPSL, CEA-CNRS-UVSQ, Université Paris-Saclay, Gif-sur-Yvette, France. ²CSIRO Oceans and Atmosphere, Aspendale, Victoria, Australia. ³Center for Ecosystem Science and Society, Department of Biological Sciences, Northern Arizona University, Flagstaff, AZ, USA. ⁴Laboratoire de Géologie, UMR 8538, Ecole Normale Supérieure, PSL Research University, CNRS, IPSL, Paris, France. ⁵INRAE, AgroParisTech, University Paris-Saclay, UMR MIA 518, Paris, France. ⁶Chair of Environmental Hydrological Systems, Faculty of Environmental and Natural Resources, University of Freiburg, Freiburg, Germany. ⁷Water Systems and Global Change Group, Wageningen University & Research, Wageningen, the Netherlands. ⁸Agroscope, Climate and Agriculture Group, Zurich, Switzerland. ⁹Geosystems Research Institute, Mississippi State University, Mississippi State, MS, USA. ¹⁰Wetland Biogeochemistry Laboratory, Soil and Water Science Department, University of Florida, Gainesville, FL, USA. ¹¹State Key Laboratory of Urban and Regional Ecology, Research Center for Eco-environmental Science, Chinese Academy of Sciences, Beijing, China. ¹²University of Chinese Academy of Sciences, Beijing, China. ✉e-mail: yuanyuanhuang2011@gmail.com

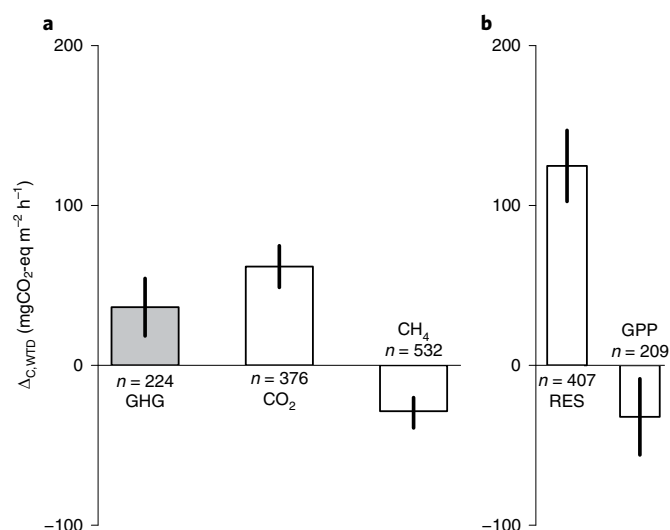


Fig. 1 | Effects of water-table drawdown on peatland CO₂ and CH₄ fluxes. **a**, The net exchange of CO₂ (NEE), CH₄ and their combination (GHG). **b**, Ecosystem respiration (or soil respiration in the absence of live plants, RES) and photosynthetic CO₂ uptake (GPP). *n* is the number of experiments. Mean effect sizes were obtained through our meta-analysis. Error bars correspond to 95% CI. The CH₄ is expressed as its CO₂ equivalence assuming its global warming potential is 25 times that of CO₂. We define a positive sign for emissions to the atmosphere and vice versa.

plant uptake of CO₂ but generally lower CH₄ emissions, the net GHG balance, therefore the global climatic impact of water-table drawdown remains highly variable^{13,14}.

In order to deal with the heterogeneity of experimental results, we conducted a meta-analysis based on random effect models to quantitatively summarize results across multiple studies. Our sign convention is a positive sign for CO₂ or CH₄ emissions to the atmosphere, and a positive sign for a water-table depth (WTD) becoming deeper. $\Delta_{CO_2, WTD}$ represents the difference of NEE resulting from a drawdown of WTD, and $\Delta_{CH_4, WTD}$ is the same for the difference of CH₄ emissions. $\Delta_{CH_4, WTD}$ is expressed as its CO₂ equivalence assuming its global warming potential is 25 times that of CO₂ over a 100-year time span³. The net GHG balance is defined by $\Delta_{GHG, WTD} = \Delta_{CO_2, WTD} + \Delta_{CH_4, WTD}$. Note here that $\Delta_{GHG, WTD}$, $\Delta_{CO_2, WTD}$ and $\Delta_{CH_4, WTD}$ vary with the magnitude of water-table drawdown.

The estimated mean value of $\Delta_{CO_2, WTD}$ (Fig. 1) is 62 mgCO₂ m⁻² h⁻¹ (47 to 77), all ranges are 95% confidence intervals (CI), meaning an increase of CO₂ emissions (or a decreased sink) for a water table becoming deeper. This estimated mean is significantly positive because the 95% CI does not overlap zero (Methods; Supplementary Fig. 3) despite individual values of $\Delta_{CO_2, WTD}$ varying from -497 to 1,234 mgCO₂ m⁻² h⁻¹ across sites (Supplementary Fig. 11). Complex responses and interactions of biotic and abiotic processes make it difficult to identify a unifying mechanism for NEE responses. Vegetation coverage, species composition, photosynthetic capacity, biomass allocation, substrate quality, nutrient availability, environmental conditions (for example, soil temperature, water availability and aeration status), peat physicochemical properties, microtopography, extent of changes in water level and experimental duration (short-term versus long-term) are possible dominant factors on NEE responses from individual experiments. Overall, water-table drawdown induced an increase in CO₂ emissions from respiration exceeding that of GPP uptake (Fig. 1b). By contrast, the estimated mean value of $\Delta_{CH_4, WTD}$ shown in Fig. 1 is -26 mgCO₂-eq m⁻² h⁻¹ (95% CI: -35, -20), revealing a significant reduction of CH₄ emissions or an increase in the CH₄ sink resulting

from decreased methanogenesis and/or enhanced methanotrophy (Fig. 1; Supplementary Fig. 3). $\Delta_{CH_4, WTD}$ across sites ranges from -1,120 to 484 mgCO₂-eq m⁻² h⁻¹ (Supplementary Fig. 11). Using data from experiments that measured both NEE and CH₄ emissions, we estimated a significantly positive mean value of $\Delta_{GHG, WTD}$ equal to 33 mgCO₂-eq m⁻² h⁻¹ (9 to 57), which implies that lowering WTD leads to a net increase of radiative forcing. The result of an overall positive $\Delta_{GHG, WTD}$ is robust and consistent among different estimating methods (Supplementary Fig. 3).

We then quantified the sensitivities of GHG fluxes to the magnitude of water-table drawdown (Δ_{WTD}), and found that the overall average sensitivity to a 1 cm water-table drawdown was 4.1 (3.3 to 5.0) mgCO₂ m⁻² h⁻¹ for CO₂ (NEE) and -2.9 (-3.6 to -2.2) mgCO₂-eq m⁻² h⁻¹ for CH₄ (Methods, Supplementary Fig. 4). The average sensitivity of $\Delta_{GHG, WTD}$ was 1.6 (0.8 to 2.3) mgCO₂-eq m⁻² h⁻¹ cm⁻¹ based on a subset of experiments that measured both NEE and CH₄. No significant pattern in the regional values of $\Delta_{GHG, WTD}$ was found (Supplementary Figs. 5–10; Supplementary Discussion), because of the large inter-site variability of the observed fluxes, small sample sizes in Arctic, tropical and coastal regions, and non-linear responses to Δ_{WTD} . The average sensitivity of $\Delta_{CH_4, WTD}$ to unit water-table drawdown was smaller (less reduction) in tropical than boreal and temperate peatlands (Supplementary Fig. 6). The difference between these regions was significant (95% CIs did not overlap) according to one of the weighting approaches considered. Respiration of coastal regions had a greater average sensitivity than non-coastal regions, while differences of NEE (or CH₄) were inconsistent (Supplementary Fig. 8). Undisturbed coastal regions are more likely to experience frequent flooding and anoxic conditions, leaving more labile peat susceptible to decomposition if the water table was lowered. Among different peatland types, the mean $\Delta_{CO_2, WTD}$ per unit Δ_{WTD} was higher in swamps than bogs and fens (not significant, Supplementary Fig. 10). Fens had higher mean $\Delta_{CO_2, WTD}$ and mean $\Delta_{GHG, WTD}$ per unit Δ_{WTD} than bogs.

Responses of GHG emissions to WTD were non-linear and covaried with peatland types, regions, land use and management histories, hydrology, vegetation characteristics, climate, and physicochemical properties of peat^{4,13,15–17}. Therefore, upscaling above-estimates to the global scale can be problematic. To further understand how different factors regulated $\Delta_{CO_2, WTD}$ and $\Delta_{CH_4, WTD}$, we built random forest models¹⁸ for these two quantities (see Methods). The random forests were built against site data using as predictors Δ_{WTD} , WTD, CO₂ (NEE) and CH₄ emissions under the high (shallow) water-table treatment (WTD_{initial}, CO_{2, initial} and CH_{4, initial} in short), climatic, topographic, edaphic, biotic, management and experimental factors (Methods; Supplementary Tables 2 and 3). We show in Fig. 2 that CO_{2, initial}, Δ_{WTD} and WTD_{initial} are the most important predictors of $\Delta_{CO_2, WTD}$, accounting for 53% of the Gini-based relative importance (Supplementary Table 4; Fig. 2; Supplementary Figs. 13 and 15). Variations in $\Delta_{CH_4, WTD}$ are mostly explained by CH_{4, initial}, Δ_{WTD} and WTD_{initial} (relative importance: 88%; Supplementary Table 5; Fig. 2; Supplementary Figs. 14 and 15). The models predict that peatlands with a stronger initial CO₂ sink capacity (CO_{2, initial}), a shallower WTD_{initial} and a larger Δ_{WTD} have a more positive $\Delta_{CO_2, WTD}$ value (Fig. 2, red lines), and that peatlands with a larger CH_{4, initial} flux to the atmosphere and a bigger Δ_{WTD} experience a stronger reduction in their CH₄ emissions, that is, a more negative $\Delta_{CH_4, WTD}$ value (Fig. 2, red lines).

By scaling up using the random forest models, we found that Arctic peatlands were more likely to have both positive and negative $\Delta_{CO_2, WTD}$ when conditions varied (Supplementary Fig. 16). The average response curves showed that Arctic peatlands were more sensitive to Δ_{WTD} and CO_{2, initial} over the whole predictor space (Supplementary Fig. 17). $\Delta_{CH_4, WTD}$ of tropical peatlands could be less or more than boreal peatlands when CH_{4, initial} varied (Supplementary

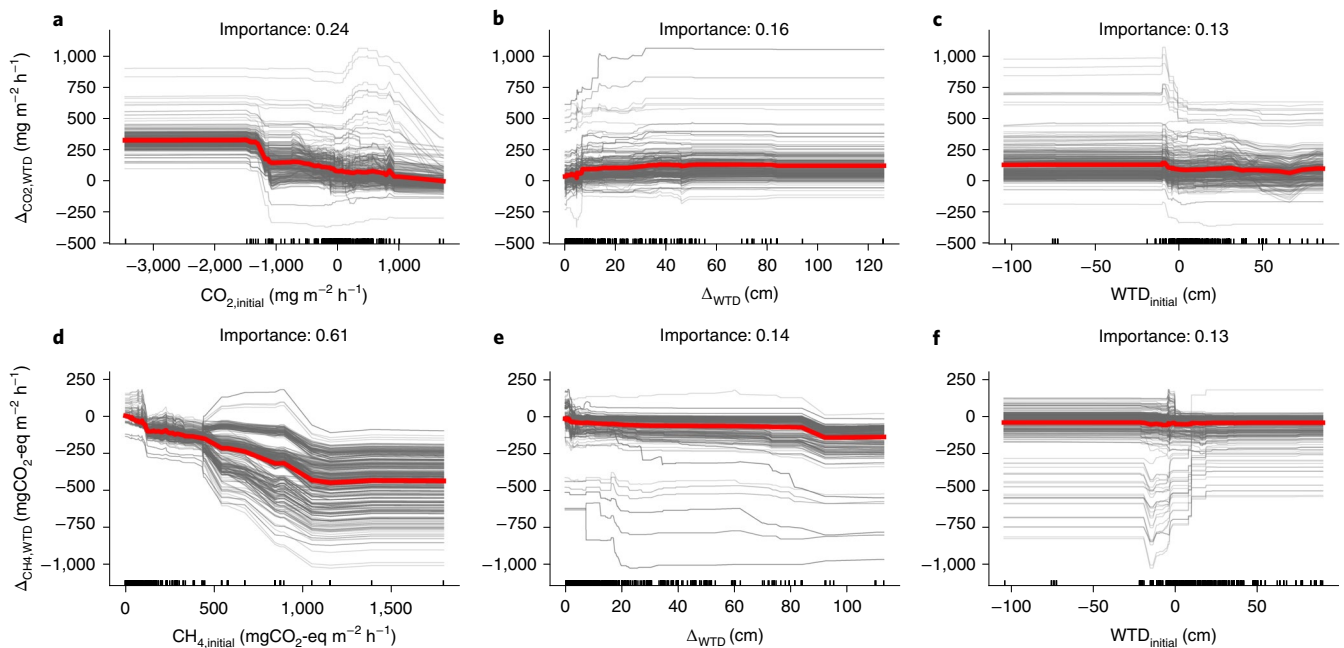


Fig. 2 | Responses of $\Delta_{\text{CO}_2,\text{WTD}}$ and $\Delta_{\text{CH}_4,\text{WTD}}$ to predictors. a–f, The graphs show how $\Delta_{\text{CO}_2,\text{WTD}}$ (a–c) and $\Delta_{\text{CH}_4,\text{WTD}}$ (d–f) respond to predictors: $\text{CO}_{2,\text{initial}}$ and $\text{CH}_{4,\text{initial}}$ (a,d), Δ_{WTD} (b,e) and $\text{WTD}_{\text{initial}}$ (c,f). One grey line captures responses per one pair of field studies to a gradual increase of the corresponding predictor while holding other predictors constant. Red lines are the averages across individual studies. We show the top three most important predictors ordered in declining importance from left to right. See Supplementary Figs. 13 and 14 for other predictors. $\text{WTD}_{\text{initial}}$, $\text{CO}_{2,\text{initial}}$ and $\text{CH}_{4,\text{initial}}$ are water-table depth, net ecosystem exchange of CO_2 and CH_4 under high water table. Δ_{WTD} is the magnitude of water-table drawdown. Rugs at the bottom indicate the distributions of predictors.

Figs. 16 and 17). Overall, both $\Delta_{\text{CO}_2,\text{WTD}}$ and $\Delta_{\text{CH}_4,\text{WTD}}$ were highly sensitive to Δ_{WTD} when Δ_{WTD} was small (<10 cm), and also became highly sensitive to $\text{WTD}_{\text{initial}}$ when $\text{WTD}_{\text{initial}}$ was around the surface. $\Delta_{\text{CO}_2,\text{WTD}}$ stayed relatively constant when $\text{WTD}_{\text{initial}}$ was 10 cm above the surface or 80 cm below the surface. $\Delta_{\text{CH}_4,\text{WTD}}$ was not responsive to $\text{WTD}_{\text{initial}}$ for strong drying or wetting when $\text{WTD}_{\text{initial}}$ got typically more than 33 cm below the surface or 21 cm above the surface (Fig. 2, Supplementary Figs. 16 and 17). That being said, the above-mentioned broad patterns that emerged from our analyses may not hold under some specific environmental conditions, due to the strong nonlinearity of response curves. Apart from these average responses, each individual paired experiment carried a unique response pattern as an outcome of complex interactions involving peatland characteristics, climate and other environmental factors (Fig. 2, grey lines; see Supplementary Figs. 13 and 14 for the responses to different factors).

Based on future WTD predicted by de Graaf et al.¹⁹ under their ‘business-as-usual’ water demand scenario and the RCP8.5 climate change scenario (Methods), we used the trained random forest models to compute global gridded CO_2 (NEE) and CH_4 emissions in response to future water-table drawdown. We found both an increase of global peatland NEE, that is, a larger CO_2 source or a smaller sink by 1.13 (95% probability interval: 0.88–1.50) $\text{GtCO}_2\text{yr}^{-1}$ and a reduction of peatland CH_4 emissions by 0.26 (0.14–0.52) $\text{GtCO}_2\text{-eq yr}^{-1}$, which together amounts to a net increase of GHG of 0.86 (0.36–1.36) $\text{GtCO}_2\text{-eq yr}^{-1}$ by 2100 (see Fig. 3 and Supplementary Figs. 21, 23, 25 and 27). This estimated net GHG budget was 0.73 (0.2–1.2) $\text{GtCO}_2\text{-eq yr}^{-1}$ under the RCP2.6 climate scenario by 2100 (see Fig. 3 and Supplementary Figs. 22, 24, 26 and 28). Under the scenario assuming a 40% less reduction of WTD than the de Graaf et al.¹⁹ prediction, the global $\Delta_{\text{GHG},\text{WTD}}$ reached 0.74 (0.5–1.29) $\text{GtCO}_2\text{-eq yr}^{-1}$. An 80% smaller reduction of WTD than the de Graaf et al.¹⁹ prediction yields a global $\Delta_{\text{GHG},\text{WTD}}$ of 0.53 (0.34–0.85) $\text{GtCO}_2\text{-eq yr}^{-1}$. The RCP2.6 climate scenario and

an 80% smaller reduction of water-table drawdown together brings the global $\Delta_{\text{GHG},\text{WTD}}$ down to 0.42 (0.22–0.74) $\text{GtCO}_2\text{-eq yr}^{-1}$. Note that these estimates do not account for anthropogenic impacts other than water-table drawdown, such as land use change or fires.

Across different latitudes, regions with high CH_4 reductions generally have high $\Delta_{\text{CO}_2,\text{WTD}}$ and $\Delta_{\text{GHG},\text{WTD}}$. Mid-to-high northern latitudes and tropics dominate the global response of GHG budgets to water-table drawdown due to their large areas (Fig. 3; Supplementary Figs. 21 and 22). Inferred from several drained peat sites in Finland, Laine et al.¹⁴ suggested a reduced GHG emission from northern peatlands under future drying because of lower CH_4 emissions and enhanced vegetation CO_2 uptake offsetting peat CO_2 emissions. We found negative $\Delta_{\text{GHG},\text{WTD}}$ over Finland (Supplementary Figs. 23 and 24). Across northern peatlands, positive $\Delta_{\text{GHG},\text{WTD}}$ outweighs negative $\Delta_{\text{GHG},\text{WTD}}$, resulting in the positive (warming) feedback on future climate. We acknowledge large uncertainties in predicting future GHG emissions over northern peatlands. In particular, permafrost thawing, a critical process that has dramatic impacts on the climate system²⁰, was not included as a predictor in our model. Arctic warming and permafrost thaw can alter peatland hydrology. Thermokarst peatlands form as a result of permafrost thaw. Thermokarst peatlands are known for their localized patchy landscape with distinguished dry–wet zones and irregular hummocks and hollows. Considering the big sensitivity of GHG to Δ_{WTD} in Arctic peatlands, widespread alterations of hydrology could dramatically change Arctic GHG budgets.

Peatlands in Scandinavia, coastal regions or along river networks are predicted to experience high reductions in CH_4 emissions in response to future water-table drawdown (Supplementary Figs. 25 and 26). Latitudinal average CH_4 reductions are higher in tropics than high latitudes. High CH_4 fluxes, relatively large change of WTD, and its warm environment make Amazonian peatlands the largest contributor to total CH_4 reduction in tropics. This prediction is subject to large uncertainties because of limited field

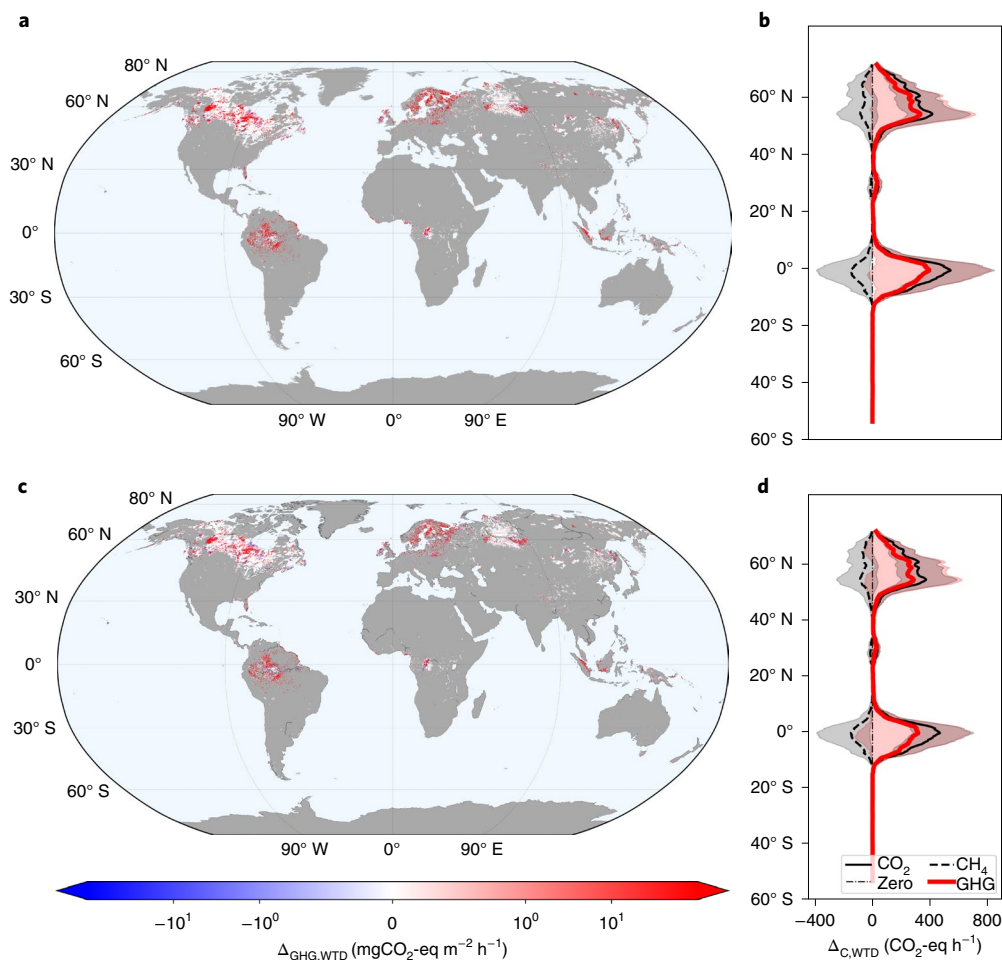


Fig. 3 | GHG changes in response to water-table drawdown by 2100. a,b, Results with RCP8.5 climatic variables. **c,d,** Results under RCP2.6. Latitudinal totals (**b,d**) were estimated through the average values per area across 0.1 degree latitude bands and peatland areas (Supplementary Figs. 21 and 22), and were smoothed with a window size of 5 degrees. Shading areas are 95% intervals. White regions show locations with small $\Delta_{\text{GHG,WTD}}$ or with negligible water-table drawdown. Spatial distributions of $\Delta_{\text{CO}_2,\text{WTD}}$ and $\Delta_{\text{CH}_4,\text{WTD}}$ are provided in Supplementary Figs. 25 and 26 and the 95% CIs in Supplementary Figs. 27 and 28.

observations in Amazonian peatlands. Few field studies in Amazonian peatlands have documented high CH_4 fluxes^{21,22}. The spatiotemporal variability, hydrologic and biogeochemical controls of CH_4 emissions across Amazonian peatlands remain poorly understood. Southeast Asian peatlands show low CH_4 emissions in comparison to temperate and boreal peatlands¹³, most likely due to poorer substrate quality (lower carbohydrate and greater aromatic content) of tropical peats²³. It remains largely unclear whether the low CH_4 fluxes are widespread across tropics, or biases from limited sample size and coverage. Boreal and temperate peatlands had experienced widespread drainage and peat conversion before the twenty-first century, while tropic peatlands are subject to large-scale disturbance in the future²⁴. The recent discovery of the world's largest tropical peatland in the Congo basin²⁵ highlights the need for additional field observations in tropics to understand hydrological controls on CH_4 emissions.

A less controversial issue in tropics is the higher CO_2 emissions following water-table drawdown. Tropical peatlands contain about 5–10% of global soil carbon²⁶. Ours and earlier¹³ syntheses (Supplementary Fig. 6) found an increase in emission of at least $10 \text{ mgCO}_2 \text{ m}^{-2} \text{ h}^{-1}$ by respiration for each 1 cm of water-table drawdown. Many tropical peatlands are occupied by swamp forests, and some of them were converted into agricultural land uses with a

lowering of the WTD, which would result in an increase in CO_2 emissions²⁷. In Southeast Asia, 25% of deforestation occurs in peat swamp forests²⁷. Water-table management and conservation of tropical swamp forests are critical for climate mitigation in the tropics, due to the high CO_2 emissions from swamp forests and the positive feedbacks among water-table drawdown, GHG emissions and climate warming. Under RCP8.5 where CO_2 emissions continue to rise throughout the twenty-first century with warmer climate conditions, global $\Delta_{\text{GHG,WTD}}$ is predicted to increase by 18% more than under the less warm RCP2.6 scenario. These estimates are rather conservative, because we did not account for the effect of lowering the water table under a warm and drying climate on $\Delta_{\text{GHG,WTD}}$. Positive contributions of water-table drawdown to GHGs accelerate future GHG emissions through climate feedback.

This study reveals that despite water-table drawdown reducing global peatland CH_4 emissions, increased CO_2 flux outweighs the climate benefits of reduced CH_4 in terms of global warming potential. Many other adverse environmental and ecological impacts associated with peatland water-table drawdown have already motivated national and international actions to preserve pristine peatlands and rewet drained peatlands. Controlling the magnitude of future water-table drawdown is an effective measure as future $\Delta_{\text{CO}_2,\text{WTD}}$ and $\Delta_{\text{CH}_4,\text{WTD}}$ are largely regulated by Δ_{WTD} (Supplementary

Tables 6–8). Rewetting to ~10 cm above-surface greatly reduces CO₂ emissions, it may also increase CH₄ emissions, especially in regions where pristine peatlands are strong CH₄ emitters. Instead of rewetting all drained peatlands, care must be taken in regional implementation, as the tradeoff between CO₂ decrease and CH₄ increase is dependent on many local factors. Climate change mitigation strategies outside peatlands that aim to limit global warming are also critical for lowering peatland GHG emissions. Finally, despite substantial progresses in peatland studies over recent decades, there are still large uncertainties in quantifying peatland CO₂ (NEE)^{28,29}, CH₄ emissions³⁰ and WTD¹⁹ dynamics over large spatial scales. Arctic, coastal and tropical regions are highly vulnerable, but largely understudied, especially in the area of long-term vegetation adaptation. Dominant control on the response of peatland carbon to water-table drawdown may also vary with timescales. As a first step, we assessed the uncertainty of our prediction through combining different datasets to account for currently known major uncertainty sources, which is yet to be all inclusive. Additional observations especially from those under-sampled regions will enable us to reduce the uncertainty in the estimated response of peatland to climate change and developing appropriate mitigation strategies in the future.

Online content

Any methods, additional references, Nature Research reporting summaries, source data, extended data, supplementary information, acknowledgements, peer review information; details of author contributions and competing interests; and statements of data and code availability are available at <https://doi.org/10.1038/s41558-021-01059-w>.

Received: 6 May 2020; Accepted: 26 April 2021;
Published online: 7 June 2021

References

1. Yu, Z. C., Loisel, J., Brosseau, D. P., Beilman, D. W. & Hunt, S. J. Global peatland dynamics since the Last Glacial Maximum. *Geophys. Res. Lett.* <https://doi.org/10.1029/2010gl043584> (2010).
2. Frohking, S. et al. Peatlands in the Earth's 21st century climate system. *Environ. Rev.* **19**, 371–396 (2011).
3. Myhre, G. et al. *Anthropogenic and Natural Radiative Forcing* (Cambridge Univ. Press, 2013).
4. Ise, T., Dunn, A. L., Wofsy, S. C. & Moorcroft, P. R. High sensitivity of peat decomposition to climate change through water-table feedback. *Nat. Geosci.* **1**, 763–766 (2008).
5. Leifeld, J. & Menichetti, L. The underappreciated potential of peatlands in global climate change mitigation strategies. *Nat. Commun.* **9**, 1071 (2018).
6. Hooijer, A. et al. Subsidence and carbon loss in drained tropical peatlands. *Biogeosciences* **9**, 1053–1071 (2012).
7. Nagano, T. et al. Subsidence and soil CO₂ efflux in tropical peatland in southern Thailand under various water table and management conditions. *Mires Peat* **11**, 6 (2013).
8. Erkens, G., van der Meulen, M. J. & Middelkoop, H. Double trouble: subsidence and CO₂ respiration due to 1,000 years of Dutch coastal peatlands cultivation. *Hydrol. J.* **24**, 551–568 (2016).
9. Swindles, G. T. et al. Widespread drying of European peatlands in recent centuries. *Nat. Geosci.* **12**, 922–928 (2019).
10. *2013 Supplement to the 2006 IPCC Guidelines for National Greenhouse Gas Inventories: Wetlands* (eds Hiraishi, T. et al.) (IPCC, 2014).
11. Wilson, D. et al. Greenhouse gas emission factors associated with rewetting of organic soils. *Mires Peat* **17**, 4 (2016).
12. Laiho, R. Decomposition in peatlands: reconciling seemingly contrasting results on the impacts of lowered water levels. *Soil Biol. Biochem.* **38**, 2011–2024 (2006).
13. Couwenberg, J., Dommain, R. & Joosten, H. Greenhouse gas fluxes from tropical peatlands in south-east Asia. *Glob. Change Biol.* **16**, 1715–1732 (2010).
14. Laine, J. et al. Effect of water-level drawdown on global climatic warming: northern peatlands. *Ambio* **25**, 179–184 (1996).
15. Prananto, J. A., Minasny, B., Comeau, L. P., Rudiyanto, R. & Grace, P. Drainage increases CO₂ and N₂O emissions from tropical peat soils. *Global Change Biol.* **26**, 4583–4600 (2020).
16. Turetsky, M. R. et al. A synthesis of methane emissions from 71 northern, temperate, and subtropical wetlands. *Glob. Change Biol.* **20**, 2183–2197 (2014).
17. Jungkunst, H. F. & Fiedler, S. Latitudinal differentiated water table control of carbon dioxide, methane and nitrous oxide fluxes from hydromorphic soils: feedbacks to climate change. *Glob. Change Biol.* **13**, 2668–2683 (2007).
18. Breiman, L. Random forests. *Mach. Learn.* **45**, 5–32 (2001).
19. de Graaf, I. E. M., Gleeson, T., van Beek, L. P. H., Sutanudjaja, E. H. & Bierkens, M. F. P. Environmental flow limits to global groundwater pumping. *Nature* **574**, 90–94 (2019).
20. Schuur, E. A. G. et al. Climate change and the permafrost carbon feedback. *Nature* **520**, 171–179 (2015).
21. Winton, R. S., Flanagan, N. & Richardson, C. J. Neotropical peatland methane emissions along a vegetation and biogeochemical gradient. *PLoS ONE* **12**, e0187019 (2017).
22. Teh, Y. A., Murphy, W. A., Berrío, J. C., Boom, A. & Page, S. E. Seasonal variability in methane and nitrous oxide fluxes from tropical peatlands in the western Amazon basin. *Biogeosciences* **14**, 3669–3683 (2017).
23. Hodgkins, S. B. et al. Tropical peatland carbon storage linked to global latitudinal trends in peat recalcitrance. *Nat. Commun.* **9**, 3640 (2018).
24. Leifeld, J., Wust-Galley, C. & Page, S. Intact and managed peatland soils as a source and sink of GHGs from 1850 to 2100. *Nat. Clim. Change* **9**, 945 (2019).
25. Dargie, G. C. et al. Age, extent and carbon storage of the central congo basin peatland complex. *Nature* **542**, 86 (2017).
26. Minasny, B. et al. Digital mapping of peatlands – a critical review. *Earth Sci. Rev.* **196**, 102870 (2019).
27. Miettinen, J., Shi, C. H. & Liew, S. C. Deforestation rates in insular Southeast Asia between 2000 and 2010. *Glob. Change Biol.* **17**, 2261–2270 (2011).
28. Gallego-Sala, A. V. et al. Latitudinal limits to the predicted increase of the peatland carbon sink with warming. *Nat. Clim. Change* **8**, 907 (2018).
29. Jung, M. et al. The FLUXCOM ensemble of global land-atmosphere energy fluxes. *Sci. Data* **6**, 74 (2019).
30. Melton, J. R. et al. Present state of global wetland extent and wetland methane modelling: conclusions from a model inter-comparison project (WETCHIMP). *Biogeosciences* **10**, 753–788 (2013).

Publisher's note Springer Nature remains neutral with regard to jurisdictional claims in published maps and institutional affiliations.

© Crown 2021

Methods

Data collection. We extracted values of GHG fluxes for NEE, ecosystem respiration (or soil respiration in the absence of live plant), GPP, CH₄ emissions, WTD and ancillary environmental variables from water-table manipulation experiments carried out through mesocosms or in situ field conditions. Mesocosm experiments normally enclose relatively large intact peat monoliths to manipulate WTD in well-controlled conditions. In situ field experiments alter WTD through draining, ditching, precipitation exclusion, flooding, building dams or groundwater extraction. Difference in $\Delta_{\text{CO}_2, \text{WTD}}$ and $\Delta_{\text{CH}_4, \text{WTD}}$ between these two types of experiments is not significant (95% CI overlap). We do not separate mesocosm experiments from experiments without peat enclosure. We treat them as different approaches to manipulate WTD. We used the ISI Web of Science database to conduct a literature search for papers published before October 2020 with query terms including ‘water table’, ‘carbon’, ‘methane’, ‘respiration’, ‘NEE’, ‘primary production’, ‘drain’ and ‘peatland’. More papers were identified through the Chinese CNKI platform. Studies included in our database were selected according to several criteria. The study should measure at least WTD and one flux of CO₂ or CH₄ under both low- and high water-table treatments over the same time period in the same geographic region and have the same natural background and land use type. Studies that compare ecosystem responses under altered water table during different time periods, for example, from Merbold et al.³¹, were not incorporated. Studies using laboratory peat columns, with synthetic/repacked soils, artificial additions (ameliorant, biochar or compost) or through incubations or have a treatment less than 1 month were also excluded. Around one-third of studies experienced water-table disturbance 10 years earlier. Some papers reported ecosystem responses to several water-table treatments at the same location. In these cases, we rearranged and paired the datasets to have different combinations of low versus high water-table treatments. For those papers reporting multiple values across several years, we compared results from meta-analysis that separates versus lumps each year’s mean response. Differences are minor, and we reported results without lumping. In total, we obtained 96 papers that cover 130 locations, mostly in the Northern Hemisphere (Supplementary Figs. 1 and 2). A pair of data points reflecting Δ_{WTD} effects on carbon flux includes target GHG data from two treatments corresponding to a low and high WTD in a specific site. In total, we have 376 pairs on NEE (CO₂), 532 pairs of CH₄, 209 pairs of GPP and 407 pairs of ecosystem respiration (or soil in the absence of live plants, RES) measurements.

For carbon fluxes, we extracted mean values of emission for each treatment, standard deviations (SD) and sample sizes from each published study. If standard error (SE) rather than SD was reported, SD was calculated from SE. For experiments that did not document SD or SE (3–20% of the experiments), we estimated the variance through scaling the mean of each experiment by the average coefficient of variation within each treatment and each GHG. We also extracted mean WTD before and after water-table manipulation and other ancillary information (Supplementary Tables 2 and 3).

Response quantification. For each pair of data points, we use the difference ($\Delta_{\text{C,WTD}}$, in units of mgCO₂-eq m⁻² h⁻¹) in the mean value (over experimental replicates) of each CO₂ or CH₄ flux under high (shallow) (\bar{C}_h) and low (deep) water table (\bar{C}_l) (equation (1)) as a metric to quantify the effect of water-table drawdown. We chose the difference instead of the odds ratio (log) to incorporate experiments in which \bar{C}_h and \bar{C}_l vary in sign.

$$\Delta_{\text{C,WTD}} = \bar{C}_h - \bar{C}_l \quad (1)$$

We conducted the meta-analysis using the random-effect model (assuming that between-study variations are randomly distributed) and the inverse variance weighting scheme³² based on the extracted values of SD and sample sizes through the Metafor package in R version 3.6.2 (ref. ³³). The between-study variance (heterogeneity, τ^2) was quantified through the restricted maximum-likelihood method³³. The 95% CI was estimated as the Wald-type (that is, normal) CI if the standardized residuals of observations are not strongly deviated from theoretical quantiles of a normal distribution. Otherwise, we applied a bootstrapping CI estimation. We randomly sampled 90% of the original datasets with replacement and estimated the mean effect 1,000 times. The 95% CI was calculated as the 2.5% and 97.5% quantiles of the 1,000 estimates in R 3.6.2 (ref. ³³). To test the robustness of our conclusion towards an overall positive or negative response, we conducted additional meta-analyses under alternative assumptions. First, we assessed whether the conclusions depended on how individual studies are weighted³⁴. We applied the fixed effect model with weighting based on the number of replicates and with a uniform weighting. For studies with sample size not published (~20%), we used the average sample size from our database for corresponding gases. For the fixed effect model, we estimated the 95% CIs of the mean response through 10,000 times bootstrapping using the bootES library³⁵. A significant asymmetry of the funnel plot indicates the bias in compiled studies, which tend to report more results with a significant response compared to studies without. We conducted an asymmetry test through the regtest function of the Metafor package. We did not detect the publication bias in the combined effect of CO₂ and CH₄ ($p=0.31$). For CO₂ or CH₄, alone, the funnel plot ($p<0.01$) is significantly asymmetrical. We corrected the publication bias through the trimfill function in Metafor. These tests, the fixed

effect models and correction of potential publication bias, pointed to consistent signs of the overall effects. The average responses are robust (Supplementary Fig. 3).

The average sensitivity of $\Delta_{\text{C,WTD}}$ to unit change of Δ_{WTD} ($\frac{\Delta_{\text{C,WTD}}}{\Delta_{\text{WTD}}}$, mgCO₂-eq m⁻² h⁻¹ cm⁻¹) was quantified similarly with the random effect model and the inverse variance weighting scheme. Note that we do not account for variance in WTD, assuming it is relatively well measured in manipulation experiments. For regional analyses, we grouped samples into Arctic (north of 66.5°N), boreal and temperate (30°N–66.5°N, 66.5°S–30°S) and tropical regions (30°S–30°N). We also compared coastal versus non-coastal regions, and among peatland types (bog, fen, marsh, swamp).

Response attribution. Water-table manipulation studies differ in peatland types, nutrient status, background climate and other experimental designs (for example, initial WTD, drainage duration and the magnitude of drainage). Combining driving factors reported from individual studies and the availability of data across studies, we tested a list of factors to understand what drive $\Delta_{\text{CO}_2, \text{WTD}}$ and $\Delta_{\text{CH}_4, \text{WTD}}$ through the random forest method. These factors include WTD and carbon fluxes under high water-table treatment (WTD_{initial}, CO_{2,initial} or CH_{4,initial}), the magnitude of water-table manipulation (Δ_{WTD}), manipulation duration (short: <1 year; medium: 1–10 years; long: >10 years), experimental type (mesocosm versus in situ), land management (managed or not), climatic, topographic (elevation) and edaphic properties (Supplementary Tables 2 and 3). Climatic factors include mean annual precipitation, mean annual temperature, wind speed, solar radiation, vapour pressure, aridity (the ratio between potential evapotranspiration and precipitation), potential evapotranspiration and a range of other bioclimatic variables characterizing the annual trend, seasonality and extreme climatic conditions. Edaphic properties involve bulk density, pH, soil carbon content, soil nitrogen, soil phosphorus, soil potassium, cation exchange capacity, base saturation, clay content, sand content, silt content and volumetric moisture content.

Random forest is an ensemble machine learning approach that generates a number of decision trees¹⁸, and is capable of capturing non-linear interactions. We sequentially added explanatory variables one at a time and selected the random forest model that yielded the highest R^2 and the lowest root mean square error (RMSE) through leave-one-out cross-validation (LOOCV). Climatic, topographic and edaphic factors that are not documented in individual studies were extracted from high-resolution data sources listed in Supplementary Table 3. For $\Delta_{\text{CO}_2, \text{WTD}}$, the selected random forest model (with LOOCV $R^2=0.52$, RMSE = 134 mgCO₂ m⁻² h⁻¹, Supplementary Fig. 11) was built through CO_{2,initial}, Δ_{WTD} , WTD_{initial}, soil nitrogen, soil carbon content, potential evapotranspiration, bulk density, volumetric water content at –10 kPa, soil pH, wind speed, soil clay content, solar radiation and elevation (Fig. 2 and Supplementary Fig. 13). The first three predictors accounted for 53% of the relative importance (Supplementary Table 4). $\Delta_{\text{CH}_4, \text{WTD}}$ are predictable (LOOCV $R^2=0.72$, RMSE = 81 mgCO₂-eq m⁻² h⁻¹, Supplementary Fig. 11) through CH_{4,initial}, Δ_{WTD} , WTD_{initial}, wind speed, soil nitrogen content, aridity, manipulation duration (Fig. 2 and Supplementary Fig. 14). The first three predictors accounted for 88% of the relative importance (Supplementary Table 5). Tropics contribute largely to CO₂ and CH₄ budgets. The small sample size of tropical studies makes building regional random forest models infeasible. Despite being built over samples around the world, the model performance is comparable between tropical samples ($\Delta_{\text{CO}_2, \text{WTD}}$, $R^2=0.49$, RMSE = 121 mgCO₂ m⁻² h⁻¹; $\Delta_{\text{CH}_4, \text{WTD}}$, $R^2=0.66$, RMSE = 48 mgCO₂-eq m⁻² h⁻¹; Supplementary Figs. 11 and 12) and the rest of the world. Earlier synthetic studies revealed that relationships between water table and peatland greenhouse emissions were modified by peatland types, region, disturbance and so on^{15,16}. We reconstructed the functional relationship between $\Delta_{\text{CO}_2, \text{WTD}}$ (or $\Delta_{\text{CH}_4, \text{WTD}}$) and different predictors for each individual study, that is, the individual conditional expectation (ICE)³⁶ (grey lines in Fig. 2). Variations among ICE curves capture the context-dependent response patterns.

Mapping future impact. $\Delta_{\text{CO}_2, \text{WTD}}$ and $\Delta_{\text{CH}_4, \text{WTD}}$ at the end of 2100 were predicted using the random forest models built above (see Methods ‘Response attribution’), with predictors such as Δ_{WTD} , WTD_{initial}, CO_{2,initial} (or CH_{4,initial}) and future climatic conditions (wind speed, solar radiation, potential evapotranspiration, aridity), assuming that edaphic and topographic factors (soil carbon, soil nitrogen, bulk density, volumetric water content at –10 kPa, soil pH, soil clay content and elevation) remain equal to their current levels due to their relatively slow change rates. Average $\Delta_{\text{CO}_2, \text{WTD}}$ and $\Delta_{\text{CH}_4, \text{WTD}}$ were estimated through different (if available) predictor datasets (see text below and Supplementary Table 3). To verify that our main results are not outcomes of overfitting, we made predictions with the top three most important predictors, which yielded a global $\Delta_{\text{GHG, WTD}}$ of 1.47 GtCO₂-eq yr⁻¹ ($\Delta_{\text{CO}_2, \text{WTD}}$: 1.59; $\Delta_{\text{CH}_4, \text{WTD}}$: –0.12). This value is larger than the prediction from the random forest model built in the previous section, and our conclusion of an overall positive $\Delta_{\text{GHG, WTD}}$ is robust. CO_{2,initial} and CH_{4,initial} from predicting datasets are within the range spanned by observation datasets used to train the random forest models (Supplementary Fig. 20 and Supplementary Table 2). We set the upper limit of Δ_{WTD} to be 300 cm. We varied this boundary value from 100 to 400 cm, and our results stayed the same, as $\Delta_{\text{CO}_2, \text{WTD}}$ and $\Delta_{\text{CH}_4, \text{WTD}}$ are not responsive to increasing Δ_{WTD} beyond 100 cm (Fig. 3b,e). Similarly, we set the upper limit of WTD_{initial} close to the upper limit of the training dataset (around

100 cm) to avoid extrapolating. $\Delta_{\text{CO}_2, \text{WTD}}$ and $\Delta_{\text{CH}_4, \text{WTD}}$ are not sensitive to $\text{WTD}_{\text{initial}}$ when WTD is deep (Fig. 3c,f). We checked that increasing this boundary value did not change our results.

Future WTDs were projected through a physically based global hydrology and water-resources model, PCR-GLOBWB, which was coupled to the global groundwater flow model (MODFLOW) with future climate forcing (HadGEM2-ES) under the RCP8.5 GHG emission scenario and ‘business-as-usual’ water consumptions from de Graaf et al.^{19,37}. By business-as-usual, per capita water demand for industry, domestic and livestock uses as well as irrigated areas were assumed to remain constant after 2010. Per unit irrigation demands vary with projected climate change. Total future water consumption varies with the projected trends in population growth and economic development. HadGem2-ES was chosen to capture the average climatic conditions predicted from GCMs within the Inter-Sectoral Impact Model Intercomparison Project (ISIMIP, <https://www.isimip.org>). RCP8.5 was used to represent climatic conditions under the worst-case scenario for future GHG emissions. This coupled modelling tracks a range of key processes that are critical in global hydrology and water-table dynamics, particularly precipitation, evapotranspiration, runoff, infiltration, surface-groundwater interactions, capillary rise, groundwater discharge, recharge and lateral flows, water-use by agriculture irrigation, industries, households and livestock, and return flows of unconsumed withdrawn water, and showed robust estimates, as compared to observations³⁷. This is considered as the best available dataset on future WTD while we acknowledge potentially large uncertainties. Δ_{WTD} is the difference between the average WTD during 2050–2100 (future) versus 1960–2010 (historical). To assess the impact of uncertainties in future Δ_{WTD} quantifications, we conducted additional predictions with future Δ_{WTD} being 0.2, 0.4, 0.6, 0.8, 1.2, 1.4, 1.6 and 1.8 of previous quantifications (Supplementary Table 8).

We used FLUXCOM NEE to estimate CO_2 (NEE) before water-table drawdown ($\text{CO}_{2, \text{initial}}$). FLUXCOM NEE merged eddy covariance and remote-sensing observations through three machine learning techniques (MARS, ANN, RF)²⁹. In addition, we incorporated an ensemble (18 in total) estimation of NEE generated by land models LPJ-GUESS, LPJML, ORCHIDEE-DGVM, ORCHIDEE, VEGAS and VISIT driven by different climate forcing within the ISIMIP framework (Supplementary Table 3). CH_4 emissions are higher over wetland compared to upland soils³⁸. We used gridded dataset from the Wetland CH_4 Inter-comparison of Models Project (WETCHIMP), which quantified CH_4 emission rate per wetland area from seven models (LPJ-Bern, CLM4Me, DLEM ORCHIDEE-ALT, ORCHIDEE, SDGVM and LPJ-WSL) to cover uncertainties in $\text{CH}_{4, \text{initial}}$ (refs.^{30,39}). Peatland is defined through the PEATMAP⁴⁰, which combines geospatial information from a variety of peatland-specific databases and histosol distributions from the Harmonized World Soil Database V1.2 (HWSD) in the regions where peatland-specific information is not available. The total global peatland area is 4.23 million km^2 from PEATMAP. We assume no changes in future peatland distribution while acknowledging uncertainties in peatland area and that future peatland area may expand or shrink with new discoveries, under future climate change or land use. We tested the duration of water-table manipulation with the manipulation variable, going from long (>10 years), medium (1–10 years) to short-terms (≤ 1 year). The impact of manipulation duration is not big, and we reported results with long-term duration.

Future climatic conditions were predicted from GCM runs driven by RCP8.5 (worst) and RCP2.6 (optimistic) emission scenarios (see ISIMIP). We chose simulations from three GCM models that is, the GFDL-ESM2M (wettest), the HadGEM2-ES (average) and the MIROC-ESM-CHEM (driest) to account for climate uncertainties. Future potential evapotranspiration (PET) and the aridity index (the ratio between precipitation and PET) were estimated using the Penman Monteith equation for a hypothetical short grass as the reference surface (Python package, PyETo, <https://github.com/Evapotranspiration/ETo>).

We applied bootstrap resampling and ensemble prediction to estimate prediction uncertainties. For $\Delta_{\text{CO}_2, \text{WTD}}$, we randomly sampled 80% of our observation samples to build one random forest model. This random model was then used to make future predictions with different combinations of predictor datasets. We repeated this bootstrap resampling, random forest model building and future prediction 200 times. In total, we had 25,200 ($200 \times 21 \text{CO}_{2, \text{initial}} \times 2 \text{WTD}_{\text{initial}} \times 3$ climate) ensemble members and we calculated the 95% probability interval as the indicator of prediction uncertainty. Bootstrap resampling provides reasonable estimation of prediction uncertainty for random forest models⁴¹ and the ensemble approach can take into account uncertainties from both random forest algorithms and predictor variables. Similarly, we conducted 8,400 predictions for $\Delta_{\text{CH}_4, \text{WTD}}$ through 200 bootstrap resamplings, 7 $\text{CH}_{4, \text{initial}}$ datasets, 2 $\text{WTD}_{\text{initial}}$ datasets and 3 climate datasets (Supplementary Table 3). To quantify contributions to future $\Delta_{\text{CO}_2, \text{WTD}}$ and $\Delta_{\text{CH}_4, \text{WTD}}$, we conducted a series of predictions (Supplementary Tables 6 and 7) through sequentially replacing

climate, Δ_{WTD} , $\text{WTD}_{\text{initial}}$ and $\text{CO}_{2, \text{initial}}$ (or $\text{CH}_{4, \text{initial}}$) by corresponding reference level datasets listed in Supplementary Table 3.

Data availability

Source datasets and global maps generated in this study are available at <https://doi.org/10.6084/m9.figshare.13139906.v3>⁴².

Code availability

Calculations were conducted through Python 3.7.3, R 3.6.2 and ferret 6.72. Data processing code and code used to generate figures are provided through <https://doi.org/10.6084/m9.figshare.13139906.v3>⁴².

References

- Merbold, L. et al. Artificial drainage and associated carbon fluxes (CO_2/CH_4) in a tundra ecosystem. *Glob. Change Biol.* **15**, 2599–2614 (2009).
- Borenstein, M., Hedges, L. V., Higgins, J. P. T. & Rothstein, H. R. A basic introduction to fixed-effect and random-effects models for meta-analysis. *Res. Synth. Methods* **1**, 97–111 (2010).
- Viechtbauer, W. Conducting meta-analyses in R with the metafor package. *J. Stat. Softw.* <https://doi.org/10.18637/jss.v036.i03> (2010).
- van Groenigen, K. J., Osenberg, C. W. & Hungate, B. A. Increased soil emissions of potent greenhouse gases under increased atmospheric CO_2 . *Nature* **475**, 214–216 (2011).
- Kirby, K. N. & Gerlanc, D. BootES: an R package for bootstrap confidence intervals on effect sizes. *Behav. Res. Methods* **45**, 905–927 (2013).
- Goldstein, A., Kapelner, A., Bleich, J. & Pitkin, E. Peeking inside the black box: visualizing statistical learning with plots of individual conditional expectation. *J. Comput. Graphical Stat.* **24**, 44–65 (2015).
- de Graaf, I. E. M., Sutanudjaja, E. H., van Beek, L. P. H. & Bierkens, M. F. P. A high-resolution global-scale groundwater model. *Hydrol. Earth Syst. Sci.* **19**, 823–837 (2015).
- Saunois, M. et al. The global methane budget 2000–2012. *Earth Syst. Sci. Data* **8**, 697–751 (2016).
- Wania, R. et al. Present state of global wetland extent and wetland methane modelling: methodology of a model inter-comparison project (WETCHIMP). *Geosci. Model Dev.* **6**, 617–641 (2013).
- Xu, J. R., Morris, P. J., Liu, J. G. & Holden, J. PEATMAP: Refining estimates of global peatland distribution based on a meta-analysis. *Catena* **160**, 134–140 (2018).
- Coulston, J. W., Blinn, C. E., Thomas, V. A. & Wynne, R. H. Approximating prediction uncertainty for random forest regression models. *Photogramm. Eng. Remote Sens.* **82**, 189–197 (2016).
- Huang, Y. et al. Supporting data for Tradeoff of CO_2 and CH_4 emissions from global peatlands under water-table drawdown. figshare. [figshare. <https://doi.org/10.6084/m9.figshare.13139906>](https://doi.org/10.6084/m9.figshare.13139906) (2020).

Acknowledgements

Y.H., P.C., D.Z., C.Q. and D.S.G. received support from the European Research Council Synergy project SyG-2013-610028 IMBALANCE-P and Y.H., P.C., D.Z., C.Q., D.S.G., B.G. and D.M. from the ANR CLAND Convergence Institute (ANR-16-CONV-0003).

Author contributions

Y.H., P.C. and L.Q. designed this study. Y.H., L.Q. and I.D.G. contributed the data. Y.H., P.C., Y.L., D.Z., D.M. and L.Q. discussed analysis methods. Y.H. conducted the analysis and drafted the manuscript. All authors discussed the results and contributed to writing the manuscript.

Competing interests

The authors declare no competing interests.

Additional information

Supplementary information The online version contains supplementary material available at <https://doi.org/10.1038/s41558-021-01059-w>.

Correspondence and requests for materials should be addressed to Y.H.

Peer review information *Nature Climate Change* thanks Dan Charman, Connor Nolan, Debjani Sibi and the other, anonymous, reviewer(s) for their contribution to the peer review of this work.

Reprints and permissions information is available at www.nature.com/reprints.